Estuaries and Coasts
DOI 10.1007/s12237-016-0074-4

Mechanisms of Storm-Related Loss and Resilience in a Large Submersed Plant Bed

Cassie Gurbisz[1] · **W. Michael Kemp**[1] · **Lawrence P. Sanford**[1] · **Robert J. Orth**[2]

Received: 8 September 2015 / Revised: 25 January 2016 / Accepted: 30 January 2016

Abstract There is a growing emphasis on preserving ecological resilience, or a system's capacity to absorb or recover quickly from perturbations, particularly in vulnerable coastal regions. However, the factors that affect resilience to a given disturbance are not always clear and may be system-specific. We analyzed and synthesized time series datasets to explore how extreme events impacted a large system of submersed aquatic vegetation (SAV) in upper Chesapeake Bay and to identify and understand associated mechanisms of resilience. We found that physical removal of plants around the edge of the bed by high flows during a major flood event as well as subsequent wind-driven resuspension of newly deposited sediment and attendant light-limiting conditions were detrimental to the SAV bed. Conversely, it appears that the bed attenuated high flows sufficiently to prevent plant erosion at its inner core. The bed also attenuated wind-driven wave amplitude during seasonal peaks in plant biomass, thereby decreasing sediment resuspension and increasing water clarity. In addition, clear water appeared to "spill over" into adjacent regions during ebb tide, improving the bed's capacity for renewal by creating more favorable growing conditions in areas where plant loss had occurred. These analyses demonstrate that positive feedback processes, whereby an SAV bed modifies its environment in ways that improve its own growth, likely serve as mechanisms of SAV resilience to flood events. Although this work focuses on a specific system, the synthetic approach used here can be applied to any system for which routine monitoring data are available.

Keywords Submersed aquatic vegetation · Storm · Flood · Feedbacks · Resilience

Communicated by Kenneth Dunton

Electronic supplementary material The online version of this article (doi:10.1007/s12237-016-0074-4) contains supplementary material, which is available to authorized users.

✉ Cassie Gurbisz
cgurbisz@umces.edu

[1] University of Maryland Center for Environmental Science Horn Point Laboratory, 2020 Horns Point Road, Box 775, Cambridge, MD 21613, USA

[2] Virginia Institute of Marine Science, College of William and Mary, Gloucester Point, VA 23062, USA

Introduction

Although intense storm events, such as hurricanes and floods, can restructure even the most robust ecosystems (Rappaport and Whitford 1999), estuaries and coasts have become particularly vulnerable over the past several decades due to degradation associated with chronic anthropogenic stressors, including eutrophication (Carpenter et al. 1998; Cloern 2001), increasing hypoxia (Diaz and Rosenberg 2008), and climate change (Najjar et al. 2010). In addition, overfishing (Jackson et al. 2001) and habitat loss (Lotze et al. 2006) threaten the biodiversity that enriches estuaries (Duffy et al. 2015). Loss of seagrasses and other submersed aquatic vegetation (SAV) beds is particularly troubling because of the valuable ecosystem services they provide (Costanza et al. 1997; Barbier et al. 2011), such as enhanced nutrient cycling (Caffrey and Kemp 1990), shoreline protection through attenuation of waves and currents (Koch 2001), and habitat and food provisioning for a host of important organisms (Orth et al. 2006; Ralph et al. 2013).

Coupled to threats from human-induced perturbations are projected increases in the frequency and intensity of extreme

Published online: 08 February 2016

storm events (IPCC 2014), which leads to the question of whether these impaired ecosystems can withstand or rebound from such events (Cardoso et al. 2008; Grilo et al. 2011). To address this concern, we need to understand the underlying mechanisms that influence the resilience of a system, which we define here as its ability to resist or quickly recover from disturbances (Folke 2006).

Previous work has documented a suite of storm-related mechanisms of SAV loss and resilience. For example, extreme currents, waves, wind, and sediment loading during storm events can break, uproot, or bury plants (Preen et al. 1995; Cabaço et al. 2008) and pulses of suspended sediment or nutrients and subsequent algal blooms can degrade water clarity, thereby decreasing the amount of light available for plant photosynthesis (Moore et al. 1997; Longstaff and Dennison 1999). Meanwhile, plant diversity may buffer against total bed loss (Lande and Shannon 1996; Reusch et al. 2005), and a number of physiological and morphological plant acclimation strategies allow for persistence despite decreased light availability (Longstaff and Dennison 1999; Maxwell et al. 2014). In addition, biophysical feedbacks, through which plant beds alter ambient physical conditions in ways that enhance their own growth, may also help plant beds absorb storm impacts (De Boer 2007). For example, healthy plant beds decrease shear stress exerted on the seabed, thereby reducing sediment resuspension and enhancing suspended particle deposition (Gambi et al. 1990; Granata et al. 2001; Peterson et al. 2004). SAV can also take up water column nutrients (McGlathery et al. 2007) and enhance nitrification and denitrification (Caffrey and Kemp 1990; Bartoli et al. 2008), thereby decreasing nutrient availability, and, in turn, algal biomass. In both cases, the plant bed, itself, acts to increase the amount of light reaching leaf surfaces (Gruber and Kemp 2010). If plant loss does occur, recovery potential depends on postdisturbance growing conditions and species-specific rates of clonal growth and seedling recruitment (Walker et al. 2006).

Despite this broad mechanistic understanding of plant responses to storm events, observed dynamics are often difficult to predict because drivers and responses are typically system-specific (Tomasko et al. 2005). For example, the environmental characteristics of a given location, including temperature and salinity, shape the composition of SAV species, which differ in their tolerance to any given stressor (Orth et al. 2010). In addition, local geographic features, such as bathymetry and proximity to tributaries can influence the relative magnitude of stressors that accompany storm events (Campbell and McKenzie 2004; Maxwell et al. 2014). Thus, detailed information about the biological and physical characteristics that are unique to a given system may help elucidate the mechanisms that drive its dynamics.

Here, we investigate the dynamics underlying the response of an SAV bed to storm events using an example from the tidal fresh upper Chesapeake Bay. In 2011, the U.S. mid-Atlantic region experienced two major back-to-back storms. The first, Hurricane Irene, traversed Maryland coastal waters on 27–28 August, producing sustained winds >15 m s^{-1} in the upper bay but relatively little rainfall. The second was a stalled tropical weather system (the remnants of Tropical Storm Lee) that generated near-record flooding for several days in early September throughout the watershed of the Susquehanna River, the largest tributary of Chesapeake Bay. Several years prior, SAV had rapidly recolonized a large shoal in an area of the upper bay, known as Susquehanna Flats, forming the largest SAV bed in the bay (Gurbisz and Kemp 2014). However, a substantial portion of the bed was lost by the fall of 2011 following the storms. In this paper, we analyze and synthesize publically available monitoring data, which we supplement with additional field samples and a simple hydrodynamic model, to infer the mechanisms driving loss and resilience of this large, dense, and continuous meadow to the 2011 storm events. Our goal is not only to interpret drivers of change in this system but also to provide an example of how this type of synthetic analysis can be used to yield insights into ecosystem dynamics.

Methods

Study Site

Susquehanna Flats, located in the tidal freshwater upper Chesapeake Bay, is a broad shoal (~1 m average depth) surrounded by deeper channels (ranging from ~2 to >6 m) and smaller shoals with narrow flanking beds along the west and north (Fig. 1). The shoals form a subaqueous delta of the Susquehanna River, which discharges, on average, 1100 m^3 s^{-1} at Conowingo Dam 16 km north of the river mouth. Historically, the flats and the general region supported dense populations of native SAV, punctuated by a rapid increase and decrease of the non-native *Myriophyllum spicatum* in the late 1950s (Bayley et al. 1978). However, SAV populations experienced dramatic decline following record flooding that accompanied Tropical Storm Agnes in June 1972 (Bayley et al. 1978). Plant aerial cover and density on the flats remained sparse until the early 2000s, when the trajectory of the large bed suddenly changed, with the bed attaining a size (~50 km^2) that may have mirrored its historic extent. This rapid recovery corresponded to enhanced water clarity during an extended dry period and modest long-term reductions in nutrient loading (Orth et al. 2010; Gurbisz and Kemp 2014). Codominant SAV species include wild celery (*Vallisneria americana*), water stargrass (*Heteranthera dubia*), Eurasian watermilfoil (*M. spicatum*), and *Hydrilla verticillata*. In the Chesapeake Bay region, these species attain peak biomass in the late summer, spreading asexually via rhizome elongation

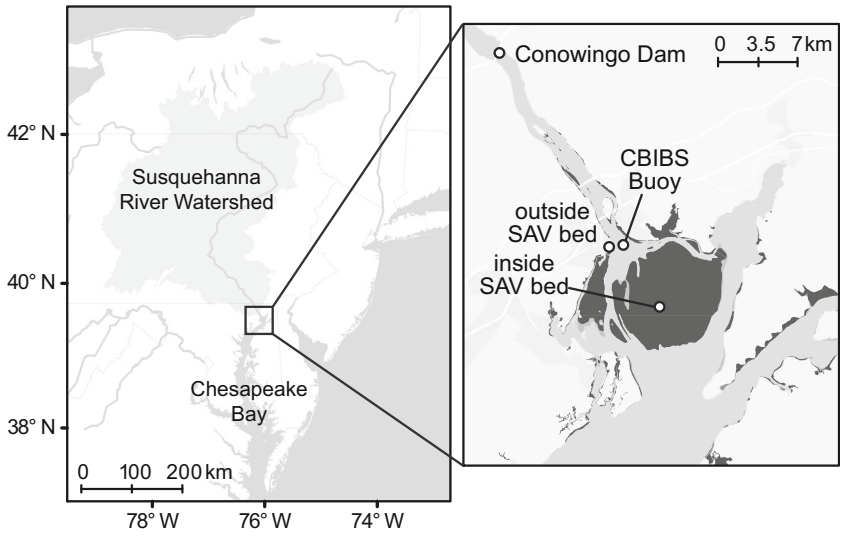

Fig. 1 The study site, Susquehanna Flats, is located in upper Chesapeake Bay near the mouth of the Susquehanna River. Water quality and plant samples were collected inside and outside the SAV bed. Wind data came from the Chesapeake Bay Interpretive Buoy System (CBIBS) buoy, and river flow data was measured at the Conowingo Dam. The SAV bed, as indicated by the *dark gray shape*, was drawn based on aerial photographs taken in 2010

from established patches, or sexually from dispersing seeds. Many of these freshwater species are also capable of dispersing and establishing from fragments (Sculthorpe 1967).

Data Sources and Collection Methods

We compiled a suite of publically available monitoring data that were collected between 2007 and 2013 at a range of sampling intervals by several agencies (Table 1). Our analyses focused on (1) annual "peak" SAV area cover and density, (2) standard water quality variables measured by the Maryland Department of Natural Resources (MDNR) at sites located inside and outside of the SAV bed, including turbidity, chlorophyll *a* (Chl *a*), total suspended solids (TSS), and the vertical diffuse downwelling attenuation coefficient (K_d), and (3) external drivers of water quality, including river discharge (measured at Conowingo Dam) and wind speed (measured at the CBIBS buoy) (Fig. 1). Sample site locations were constrained by the fact that the monitoring data had already been collected independent of this project. We calculated SAV bed area weighted for plant density using a multiplier based on median values of crown density categories (<10 %; 10–40 %; 40–70 %; 70–100 %) to estimate an index of total plant biomass, which we call "bed abundance" (Moore et al. 2000; Rybicki and Landwehr 2007). All SAV data and analyses presented in the text are for the large central bed occupying the shoal; however, the maps and time series plot presented in Fig. 1 also include smaller flanking beds.

We supplemented these monitoring datasets with additional field samples following the two storms in 2012–2014. We collected replicate plant samples near the water quality monitoring sensor inside the SAV bed at monthly intervals starting in July in 2012 and May in 2013 and ending in October each year. We also collected biomass samples in August 2014. Number of replicates varied ($n = 3$–10) to account for patchy SAV cover early in the growing season (5–10 replicates) and relatively homogeneous plant cover during peak plant biomass (3 replicates). We sampled plant material to a sediment depth of ~20 cm with an acrylic corer (15.5 cm diameter, 35 cm long) and washed each sample to remove sediment. We separated samples into aboveground and belowground living tissues and oven dried them at 60 °C to constant weight (~24–48 h). To measure epiphytic material, we collected three replicates of ~10-cm apical sections for each of the dominant species present at each biomass sampling location by placing a plastic bag over individual shoots underwater to obtain a bag containing the plant segment, associated epiphytic material, and ambient water (Twilley et al. 1983). We washed any epiphytic material that had not already detached from plant leaves into the bag containing ambient water for each sample. We filtered the water onto preweighed 45-mm glass fiber filters, which we then dried and weighed. We also dried and weighed

Table 1 Summary of publically available data sources

Data description	Source	Duration	Frequency
Water quality	Maryland Department of Natural Resources http://mddnr.chesapeakebay.net/eyesonthebay/	2007–present	4–6 h^{-1}
SAV cover	Orth et al. http://web.vims.edu/bio/sav/index.html	1984–present	1 y^{-1}
River discharge	United States Geologic Survey http://waterdata.usgs.gov/usa/nwis/uv?01578310	1967–present	1 h^{-1}
Meteorological	Chesapeake Bay Interpretive Buoy System http://buoybay.noaa.gov/locations/susquehanna	2008–present	4–6 h^{-1}

plant segments to obtain a measure of epiphyte mass per unit plant biomass.

We also measured key water quality variables at several additional stations when plant biomass was collected in 2012–2013 as well as along a transect in August 2014 four times during a tidal cycle starting in the middle of the plant bed and ending ~1.5 km south of the plant bed. For each sample, we passed a measured water volume through preweighed and ashed filters (45 mm GFF), which we then rinsed with deionized water to remove salts. We dried and weighed the filters to determine TSS concentrations. We analyzed additional filters for Chl *a* concentrations. The filters were extracted in the dark with 90 % acetone, sonicated, filtered, and read on a fluorometer (10-AU, Turner Designs). We measured dissolved inorganic nitrogen (DIN) and dissolved inorganic phosphorous (DIP) in the filtered water colorimetrically (Shimadzu UVmini-1240) (Parsons et al. 1984). In addition, we measured vertical profiles of photosynthetically active radiation (PAR) at select stations using a scalar (4pi) quantum sensor (Li-Cor) to compute K_d. We also measured turbidity, Chl *a*, dissolved O_2, pH, temperature, and salinity at each site using a YSI 6600 sensor package.

Statistical Analyses

Our overall data analysis approach was to characterize how the system changed after the extreme weather events that occurred in 2011 and to determine relationships among physical, chemical, and biological variables to explore potential drivers of change in the system.

To describe change in properties of the plant bed, we tested for differences in monthly mean plant and epiphyte biomass between 2012, 2013, and 2014 using Student's *t* test. We also tested whether plant loss based on annual aerial surveys flown in late summer (Orth et al. 2010) was related to location within the plant bed and April–September maximum river discharge. To conduct this analysis, we calculated distance from the edge of the large central plant bed as a measure of location within the bed. Using ArcGIS software, we created a grid of equally spaced (500 m) sampling points on top of each SAV bed polygon for years during which SAV loss occurred (2003, 2006, 2009, 2011), as well as each previous year. We excluded 2012 because, although there was plant loss, maximum discharge was only 2860 $m^3\ s^{-1}$. We suspect, as discussed below, that the effects of the 2011 flood event carried over into 2012 and caused additional plant loss despite relatively low flow conditions that year. We measured the distance from each point to the perimeter of the plant bed prior to loss, and we recorded the points at which plant loss occurred between years. We then used logistic regression, which is commonly applied for binary (e.g., plant loss, no plant loss) response variables (Hosmer and Lemeshow 2000), to analyze the relationship between the probability of SAV loss, distance from the outer edge of the plant bed, and maximum river discharge. We used the Pearson χ^2 test to assess model fit, in which a significant *p* value indicates evidence for lack of fit.

We investigated the magnitude of change in water quality across time and space by calculating monthly mean differences between paired (inside vs. outside the bed) continuous monitoring observations of turbidity and Chl *a*. We used bootstrap resampling (resamples = 1000) with corrected accelerated percentiles (Efron 1987) to calculate 95 % confidence intervals for the mean differences (confidence intervals that include 0 indicate no difference in means). We also used Student's *t* test to test for differences in nutrient (DIN, DIP) concentrations inside and outside the plant bed before and after the 2011 flood event in both spring and summer.

We used ordinary least squares linear regression to model relationships among TSS, YSI Chl *a*, turbidity, and K_d with data from concurrent grab samples measured at or near established stations located inside and outside SAV bed. In addition, because K_d is only measured 2–4 times per month, we used these relationships to estimate a more detailed K_d time series derived from continuous April–October Chl *a* and turbidity data spanning 2010 to 2013 at the SAV bed monitoring site. We then used this time series to calculate percent of surface light through the water (PLW) at 1 m depth using the Lambert-Beer relationship ($PLW = 100*e^{-Kd*z}$, where z = water depth) to show how the light environment changed over time inside the SAV bed. To account for additional light attenuation by epiphytic material, we used monthly epiphyte data, where available, to estimate percent light at the leaf surface (PLL) according to the methods outlined in Kemp et al. (2004).

We also estimated net ecosystem production (NEP) at the same site using continuous oxygen, temperature, and wind speed data following previously published methods (Caffrey et al. 2014; Howarth et al. 2013). Because the plants appear to be the dominant organism at this site in terms of biomass, we assume that NEP is primarily a measure of SAV metabolic activity. We can therefore use NEP to illustrate shorter timescale changes in bed productivity and investigate potential mechanisms of change in production, such as light limitation. We used linear mixed-effects models to test for differences in monthly mean NEP and the variables that affect NEP (viz., PLW, insolation, and temperature) between 2010, when the bed was at its prestorm peak, and subsequent poststorm years (2011 to 2013). The model tested for differences in the intercept (i.e., mean) given year and month. Mixed models are preferential in this case over analysis of variance or time series methods because they can explicitly account for correlation structure that is inherent in time series data and also handle large spans of missing data (Pinheiro and Bates 2000), which occurred here during winter months when monitoring sensors were removed from the water. We used bootstrap resampling

to construct 95 % confidence intervals for the differences in means (Efron 1987).

We also used a linear mixed-effects model to (1) explore the extent to which river discharge and wind speed were related to turbidity at inside and outside the SAV bed sites and (2) to test whether the effect of wind speed changed after the fall 2011 flood event. Log-transformed turbidity was the response variable. Fixed effects were river discharge and wind speed, and random effects included wind speed in relation to (1) the 2011 flood event (before, after), (2) season (spring = April–June; summer = July–September), and (3) site (inside or outside the SAV bed). We initially also included wind direction; however, its effect was not significant, so we excluded it from the model. We constructed a series of simplified models by excluding the random effects one at a time, and we compared these models to the full model to determine whether each variable improved model fit (Laird and Ware 1982). We then used bootstrap resampling to construct 95 % confidence intervals for differences between relevant random coefficients (i.e., differences in the effect of wind speed on turbidity across sites and seasons before and after the flood event).

In all cases, we checked that raw data and model residuals met test assumptions (e.g., normality, independence, and heteroskedasticity), and we made relevant transformations (e.g., log transformation) as necessary.

Hydrodynamic Model

We also developed a simple hydrodynamic model based on the same principles as the models of Fagherazzi et al. (2003) and Mariotti and Fagherazzi (2013) in an effort to strengthen our hypotheses and to provide surrogate data for variables that we believed were important but missing. The model simulates flow and bottom stress in an idealized embayment system with geometry that is broadly based on the lower Susquehanna River and Susquehanna Flats region, assuming constant river flow interacting with a standing wave tide. It was developed for a constant width channel (6 m deep) adjacent to variable width subtidal flats (1.5 m deep) with and without SAV. The model solves first for the longitudinal flow changes required to conserve water volume as the tide rises and falls and as the subtidal flats widen and narrow. Flow is then partitioned between the channel and the flats to account for the differing influences of friction on flow over the channel and the shoal, assuming a slowly varying steady state shallow water balance between horizontal pressure gradient and vertical stress gradient. In the absence of SAV, the bottom drag coefficient is the same everywhere. In the presence of SAV over the flats, the drag is increased following the methods of Chen et al. (2007), with a user-specified ratio between the channel and flats drag coefficients simulating the effects of different plant densities. Finally, the lateral flows between channel and flats are adjusted to reestablish volume conservation. The fraction of the drag responsible for sediment transport (the "skin friction") is calculated following the methods of Chen et al. (2007) as well. More model details are available in Appendix A.

We used the open-source software package R to carry out statistical analyses, run the model, and generate plots.

Results

Density-weighted plant cover ("bed abundance") of the large central bed decreased by 43 % between 2010 and 2011, then by another 20 % in 2012, followed by slight (~1 %) recovery in 2013 (Fig. 2). Logistic regression showed that the probability of plant loss decreased with distance into the plant bed and increased as river discharge increased (Table 2). There was also a significant positive interaction between distance into the plant bed and river discharge. In other words, most plant loss occurred around the outer edge of the plant bed, and higher flows led to greater overall plant loss (Fig. 3a); however, the proportion of loss at any given distance from the edge of the bed increased nonlinearly as river discharge increased (Fig. 3b). In addition, plant biomass in August and September was significantly greater in 2013 than in 2012 (Table 3, Fig. 4a) and possibly also in August 2014 compared to 2012 ($p = 0.05$). There was no significant difference between biomass in August 2013 and 2014 nor were there any significant differences in belowground biomass between years. August, September, and October epiphyte biomass levels were significantly less in 2013 than in 2012 (Fig. 4b).

NEP was lower during the spring of 2011–2013 and greater in summer of 2012–2013 compared to NEP calculated before the storm events in 2010, as indicated by 95 % confidence intervals for differences in monthly means (i.e., mixed model intercepts) that did not include 0 (Fig. 5a, e). Peak NEP occurred 1 month later in 2011 compared to 2010 and 2 months later in 2012 and 2013. PLW was generally lower after the storm events compared to 2010 (Fig. 5b, f) and, for years when epiphyte data were collected (2012 and 2013), epiphyte cover increased PLW by 15 %. However, despite overall lower light levels compared to 2010, PLW during the summer of 2011–2013 and PLL in 2013 still exceeded 30 % for a portion of the growing season. There were no differences in insolation after the flood event (Fig. 5d, h) and, although temperature was different from prestorm means during some months, these differences did not appear to systematically coincide with differences in NEP (Fig. 5g–h).

In general, monthly mean turbidity before 2011 was lower inside the plant bed compared to a nearby monitoring station located outside the plant bed (Fig. 6a). For several months following the fall 2011 storm events and into spring of 2012, turbidity was greater inside the plant bed by ~10–30 turbidity

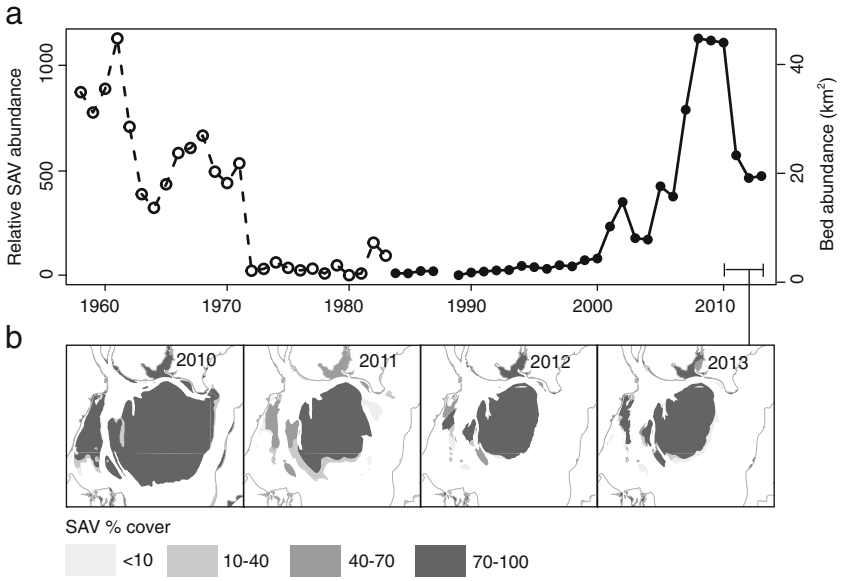

Fig. 2 **a** Time series of SAV bed abundance (1958–2013). Data from 1958–1983 (*open circles*) represent relative SAV abundance data derived from field sampling by Bayley et al. 1978 and the Maryland Department of Natural Resources (*unpubl.*). Data for 1984–2013 (*solid circles*) represent SAV abundance data derived from aerial imagery. We concatenated the time series visually to the best of our ability; however, it is important to note that they are based on different measurement scales. **b** Maps of Susquehanna Flats showing SAV spatial distribution and density cover (*shades of grey*) before (2010), immediately after the September 2011 flood event (2011), and 2 years following the event (2012–2013)

units. The difference was much less (0 to 1 NTU) during late summer–early fall 2012. Turbidity was again greater inside the plant bed by ~10 to 15 NTU in spring 2013 but then it decreased by ~5 NTU inside the plant bed in summer 2013. Monthly mean water column Chl *a* was also consistently lower inside the plant bed by ~3–7 μg l^{-1} before 2011 (Fig. 6b). Chl *a* was generally lower inside the plant bed in spring and summer of 2011 as well but by only ~1 μg l^{-1}. However, in spring and early summer of 2012 and May of 2013, Chl *a* was ~5–10 μg l^{-1} greater inside the plant bed. Seasonal peaks in Chl *a* after the flood event appear to lag those of turbidity by ~1–2 months. Regression analysis showed that TSS (but not Chl *a*) was a statistically significant predictor of turbidity (Fig. 7). Together, turbidity and Chl *a* measured by monitoring sondes predicted K_d by the following formula: $K_d = 0.95 + 0.08 * \text{turbidity} + 0.03 * \text{Chl } a$ ($p < 0.001$, $R^2 = 0.74$). Mean summer DIN increased from 0.62 ± 0.29 to 13.63 ± 4.73 μmol l^{-1} inside the plant bed; however, this difference was not statistically different [t(5.12) = −1.87, $p = 0.12$], nor were any other comparisons of DIN or DIP before and after the flood event.

Visual examination of turbidity, river discharge, and wind speed time series suggests that both river discharge and wind had an effect on turbidity, but the wind effect increased inside the plant bed after the flood event (Fig. 8). For example, although Hurricane Irene generated high sustained winds, turbidity only increased marginally both inside and outside the plant bed. During the flood event, however, turbidity increased dramatically, exceeding 600 NTU at both sites. After the flood, turbidity was, at times, more than 250 NTU greater inside the plant bed compared to the monitoring site outside the bed, particularly during wind events. Results from the linear mixed model support these inferences. Susquehanna River discharge and wind speed each had a significant positive effect on turbidity (Table 4). Including timing in relation to the flood event, site, and season improved model fit, meaning that these variables modified the effect of wind speed on turbidity. Specifically, the effect of wind speed on turbidity increased inside the bed after the flood event (95 % confidence interval (CI) for the difference in coefficients = 0.0005, 0.0019), the effect was less in the summer compared to the spring (CI = −0.0023, −0.0006), and the effect in the spring was greater inside the bed compared to outside the bed (CI = 0.0012, 0.0022).

Table 2 Logistic regression results showing distance from the outer edge of the plant bed and April–September mean river discharge as predictors of the probability of plant loss

Predictor	Coefficient	SE	*Z*	*p*
Constant	−3.40	0.96	−3.59	**<0.001**
Distance	9.2×10^{-3}	3.3×10^{-3}	−2.83	**<0.01**
Discharge	2.0×10^{-3}	5.1×10^{-4}	3.91	**<0.001**
Distance/discharge	3.6×10^{-6}	1.6×10^{-6}	2.28	**<0.05**
Overall model fit		χ^2	*df*	*p*
Hosmer-Lemeshow test		8.14	8	0.4200

The non-significant *p* value for overall model fit shows that there is no evidence for lack of fit. Bold: $p < 0.05$

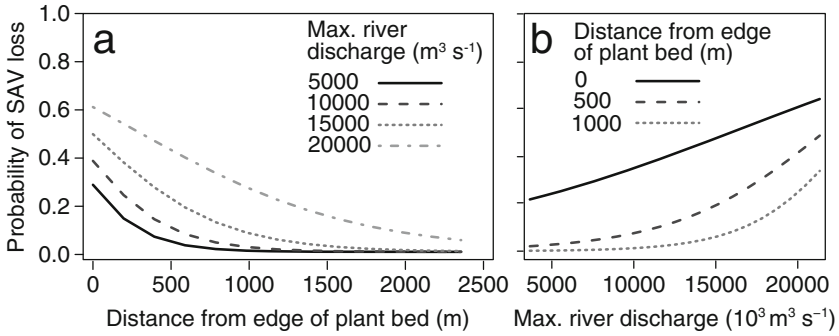

Fig. 3 Effect of the interaction between distance from the edge of the plant bed and April–September mean river discharge on probability of SAV loss. Trend lines were determined by logistic regression analysis

Water quality transect data show that by August 2014, turbidity, and thus suspended particle concentrations, was generally lower inside the plant bed (Fig. 9a–c). At high tide, turbidity inside the bed slightly increased starting around 500 m from the edge of the bed (Fig. 9b). However, at low tide, turbidity was consistently low to the edge of the bed and slightly lower for ~800 km beyond the outer edge of the bed compared to values measured at the same sites at high tide (Fig. 9c). Lower turbidity around the southern outer edge of the bed is consistent with the apparent clear water plume emanating from the bed (Fig. 9a). PLW, calculated using depth at mean water and an estimate of K_d derived from turbidity and Chl *a* data collected at transect sites, was highest in the inner core of the plant bed, slightly lower around the inner and outer edge of the bed, and lower around the southern end of the transect, where the water was both deeper and more turbid (Fig. 9d–e).

Model simulations for cases with and without the SAV bed on the flats with flow based on peak Susquehanna River flow in September 2011 (20,000 m^3 s^{-1}) at maximum ebb tide show that even in the absence of SAV, the flow and bottom stress over the flats were much lower than in the channel (Fig. 10). Minimum flows and bottom stresses generally occurred in the wide central region of the shoal, intermediate values occurred in the northern and southern narrow regions of the shoal, and the greatest values occurred in the northern river channel and the southern exit channel. When SAV were present, they greatly increased the total drag coefficient over the shoal, which greatly decreased flow over the shoal and enhanced flow in the channel (i.e., the flow pattern without SAV is greatly exaggerated with SAV). As a result, skin friction (the stress acting on the bottom sediments) was greatly reduced relative to the no SAV case. Without SAV, the minimum and maximum bottom stress values on the shoal were 1.4 and 3.2 Pa, respectively, but in the presence of SAV, skin friction on the shoal varied between 0.1–0.3 Pa. It is important to note that the total stress over the shoal with SAV remains similar to the no SAV case; the difference is that the drag of the plants dominates the total stress in the SAV case, while the drag of bottom sediments dominates the total stress in the no SAV case.

Discussion

In contrast to the near-complete SAV loss that resulted from Tropical Storm Agnes in 1972, the persistence of large portions of the bed on Susquehanna Flats and its beginnings of recovery in 2013 following two severe storms in August and September 2011 demonstrates its resilience to a strong perturbation. Our analysis of a number of monitoring parameters, additional field studies, and modeling suggests that several critical biophysical interactions between the bed and its environment coupled to the physical characteristics of the region allowed the bed to survive and start to recover, particularly after the September 2011 flood event, which produced near-record flow and sediment loading rates.

Table 3 Differences in monthly mean plant and epiphyte biomass between years

Sample dates	*t*	*df*	*p*	2012 mean	2012 SD	2013 mean	2013 SD
Above ground plant biomass							
August	−2.54	7	**<0.05**	60.69	14.36	146.10	93.63
September	−2.42	12	**<0.05**	71.68	48.01	195.89	149.97
Epiphyte biomass							
August	2.21	14	**<0.05**	2.12	3.41	0.18	0.19
Septmeber	2.54	26	**<0.05**	0.91	0.75	0.42	0.37
October	4.11	20	**<0.01**	1.02	0.78	0.23	0.18

Student's *t*-test was used to test for differences in June–October above and belowground plant biomass as well as epiphyte biomass between 2012–2013, 2012–2014, and 2013–2014. Only statistically significant results are shown. Bold: $p \leq 0.05$

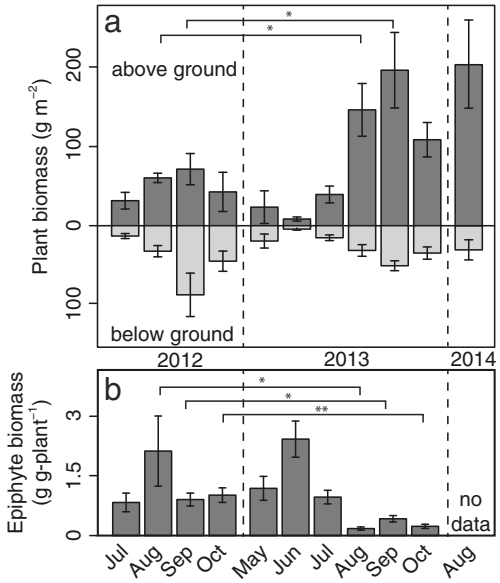

Fig. 4 2012–2014 monthly **a** plant and **b** epiphyte biomass. *Asterisks* indicate a significant difference at the 0.05 (*) and 0.01 (**) levels

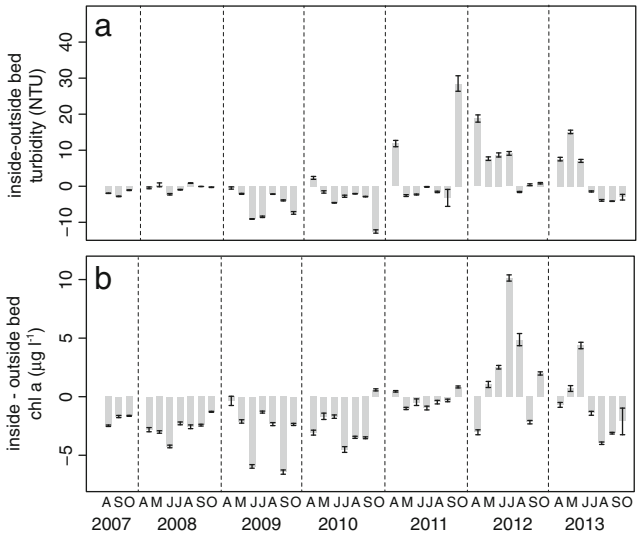

Fig. 6 Mean monthly differences ±95 % confidence interval between measurements made inside and outside the plant bed (i.e., daily measurements at the outside the bed site were subtracted from those made inside the bed and those daily differences were averaged for each month) for **a** turbidity and **b** Chl *a*

Resistance to Sediment Loading

While poor water clarity associated with particle deposition and subsequent resuspension likely caused some plant loss and decreased plant production during and after the September 2011 flood event, it appears that reduced sediment resuspension during periods of peak biomass in 2012 and 2013 led to improved water clarity. We argue that this positive feedback between the plant bed and suspended particle concentrations served as a mechanism of bed resilience to high rates of sediment loading generated by the flood.

Before September 2011, turbidity and planktonic Chl *a* were lower inside the plant bed (Fig. 5a, b), a pattern consistent with previous studies (Moore 2004; Gruber and Kemp 2010; van der Heide et al. 2011). In contrast, higher turbidity

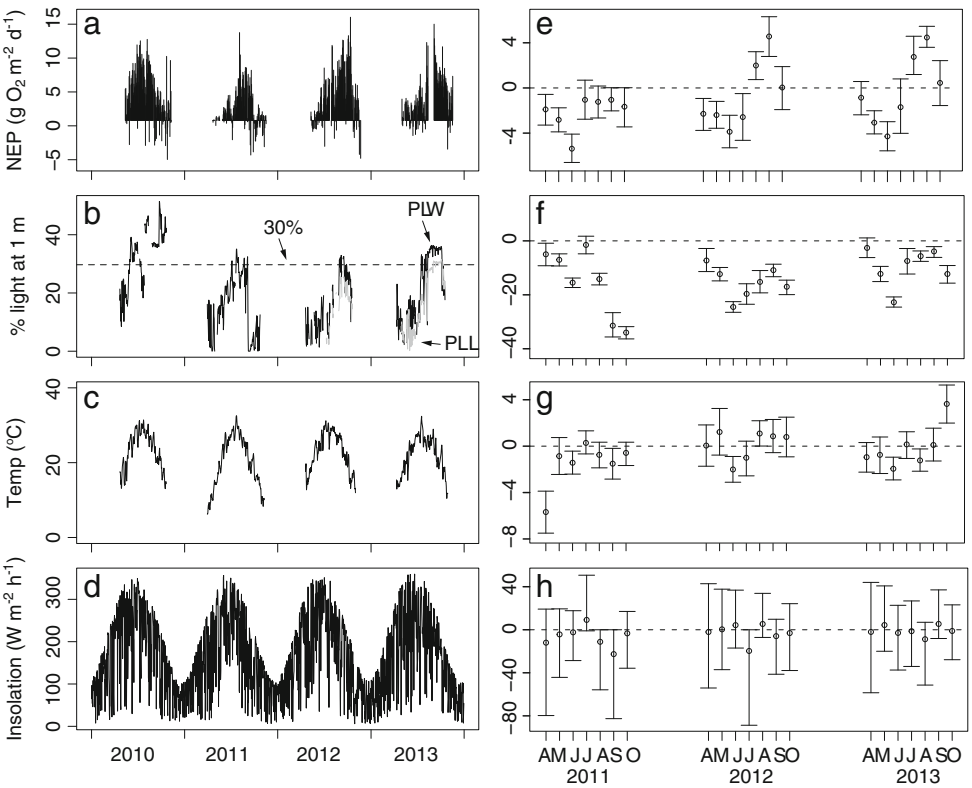

Fig. 5 **a**–**d** Time series for daily net ecosystem production (NEP) and variables that may control NEP. **e**–**h** Differences between 2010 and 2011–2013 monthly means for the same variables with 95 % confidence intervals, which were calculated by bootstrapping linear mixed-effect model coefficients. Intervals that include 0 indicate no difference

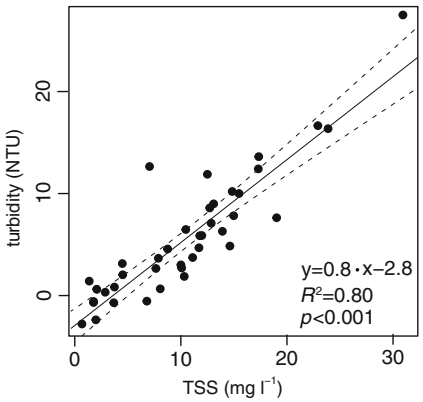

Fig. 7 Relationship between total suspended solids (TSS) and turbidity

inside the plant bed during the months immediately after the flood event in September 2011 and the subsequent two springs suggests that the flood had a lingering effect on suspended particle concentrations. Elevated Chl *a* inside the plant bed during late spring and early summer in 2012 and 2013 and greater epiphyte biomass in 2012 compared to 2013 (Fig. 4b, Table 3) imply effects on algal production as well. Because K_d, which is indicative of the amount of light available to plants, was related to both turbidity and planktonic Chl *a*, greater than normal values of these variables inside the plant bed after the flood event could have negatively affected the plant bed through light limitation.

Although the plants, on average, received enough light to survive through 2011–2013, as April–October median PLW and PLL at 1 m depth were >13 and 9 %, respectively (Dennison et al. 1993; Kemp et al. 2004), episodic extremes in turbidity that were not captured by data aggregated across the growing season could have caused plant mortality, particularly around the deeper outside and southern edges of the SAV bed (Moore et al. 1997; Longstaff and Dennison 1999). For example, PLW was <3 %, a lethal light level for most freshwater macrophytes (Middelboe and Markager 1997), for ~1 week during the September 2011 flood event and for periods of one to several days throughout the following spring (Fig. 5b). In addition, light limitation could have altered plant phenology and limited plant production. For instance, PLW was <30 %, the threshold light level below which production in these plants generally decreases (Blackburn et al. 1961; Harley and Findlay 1994), until July–August in 2012 and 2013. Light limitation early in the growing season could, thus, account for the apparent delay of annual peak production (Fig. 5a). Furthermore, because summer PLW and PLL were generally higher in 2013 compared to 2012, lower production rates associated with light limitation may also be responsible for lower biomass in 2012.

However, despite unusually poor springtime water clarity inside the plant bed after the flood event, light conditions improved by late summer in 2012 and 2013. Concurrent temporal patterns in plant biomass, turbidity, and Chl *a* suggest that the bed itself caused this improvement. For example, turbidity and Chl *a* decreased (Fig. 6) and PLW increased inside compared to outside the plant bed by August in 2012 and July in 2013 (Fig. 5c). These patterns coincided with increases in monthly plant biomass to 55 g m^{-2} and 41 g m^{-2} respectively (Fig. 4), suggesting that after accumulating sufficient plant volume, the bed improved water quality and increased light availability, thereby allowing for increased plant production during the summer months.

Our analyses indicate that greater than usual wind-driven resuspension in the absence of plants and reduced resuspension when plants were present generated the observed patterns in turbidity. Because turbidity was related to both TSS (Fig. 7) and wind speed (Table 4), we can infer that higher wind speeds, in general, led to greater concentrations of suspended particles. The increased effect of wind on turbidity inside the plant bed during the spring after the flood (Fig. 8) further

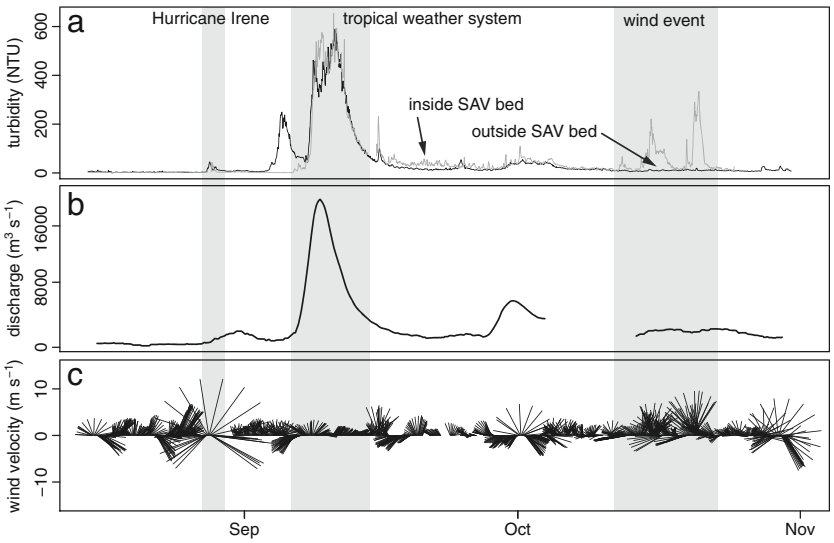

Fig. 8 Time series for **a** turbidity measured inside (*gray*) and outside (*black*) the plant bed, **b** 2-day moving average of Susquehanna River discharge measured ~16 km upriver at Conowingo Dam, and **c** wind velocity measured at the mouth of the Susquehanna River and smoothed using a 13-h moving average

Table 4 Relationships between environmental variables and turbidity, as shown by linear mixed-effects regression models

Fixed effect parameter estimates						
Predictor	Estimate	SE	*t*	*p*		
Discharge	0.00020	0.00002	9.854	<0.0001		
Wind speed	0.00056	0.00027	2.091	<0.05		
Effect of random terms						
Model	*df*	*AIC*	*BIC*	Log-likelihood	Likelihood ratio	*p* value
Maximal	13	189	253	−81		
Maximal—site	10	460	509	−220	277.2	<0.0001
Maximal—timing	10	584	633	−282	401.1	<0.0001
Maximal—season	10	566	616	−273	383.4	<0.0001
Maximal—slope (wind speed)	7	242	276	−114	65.0	<0.0001
Maximal + AR1	14	−605	−536	317	795.8	<0.0001

Fixed effect predictor variables include Susquehanna River discharge and wind speed. Random effects include timing in relation to the September 2011 flood (before or after), site (inside or outside the SAV bed), and season (spring = April, May, June; summer = July, August, September). Random effects were sequentially removed to investigate whether each significantly affected model fit. Model improvement by including first order autoregressive (AR1) correlation structure is also demonstrated

suggests that the September 2011 flood event created an environment on the shoal in which bottom sediments were highly resuspendible, probably due to substantial deposition (Palinkas et al. 2013) of loose, unconsolidated sediment (Ward 1985; Sanford 1994; Sanford 2008) and creation of open scour channels by high flows (Luhar et al. 2008). Subsequent wind events then generated turbid conditions through resuspension by wind-forced waves, particularly during the spring when plants had yet to germinate or had just begun to emerge. However, the diminished effect of wind on turbidity during the summer when plant biomass was high (Fig. 4) implies a bed effect on turbidity. In general, the vertical transfer of turbulent stress to the seabed and thus sediment resuspension decreases when canopy drag surpasses a critical threshold due to increasing plant height and density (Ward 1985; Luhar et al. 2008; Gruber et al. 2011). Therefore, it appears that once the bed reached a critical biomass, canopy drag dissipated wind-driven wave energy and stabilized the seabed, thereby allowing more light to reach the leaf surface to support photosynthesis (De Boer 2007; Chen et al. 2007).

Similar patterns in Chl *a* (Figs. 4b and 6b) and higher epiphyte biomass in the summer of 2012 compared to 2013 suggest that increased inputs of particle-bound nutrients and subsequent resuspension events may also be linked to greater than normal planktonic and epiphytic algae production in 2012 and early 2013. Although differences in DIN and DIP before and after the flood event were not statistically significant, the increase in summer DIN inside the plant bed

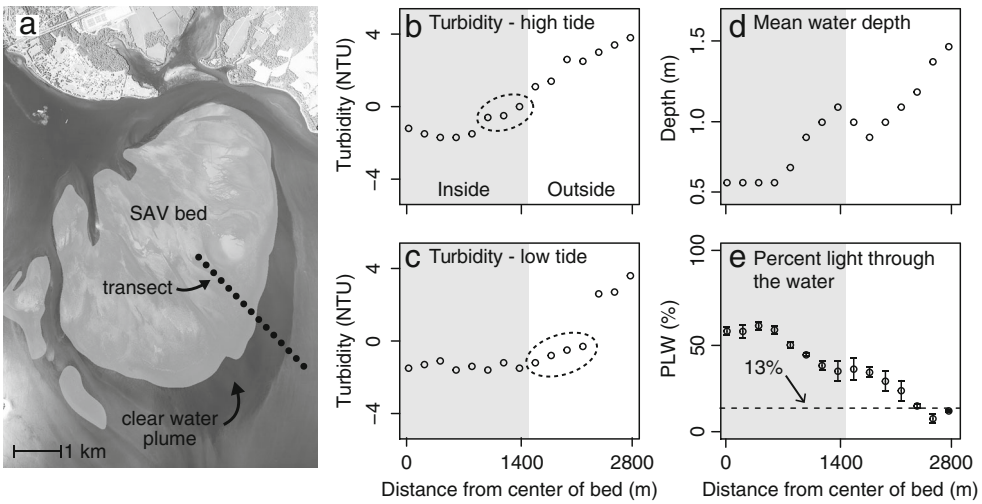

Fig. 9 **a** Aerial photo of the SAV bed in 2013 (shaded *light gray*), the "plume" of clear water emanating from its southern edge, and water quality transect sampling sites (*black dots*). **b**, **c** Turbidity data for high and low tide, respectively. *Dashed circles* indicate areas of increased turbidity in the inner edge region at high tide and lower turbidity immediately outside the plant bed at low tide. **d** Mean water depth at transect sites. **e** Percent light through the water (PLW) calculated using turbidity and Chl *a* (to estimate K_D) and depth data. Thirteen percent, indicated by the *dashed line*, is the minimum light requirement for upper Bay SAV

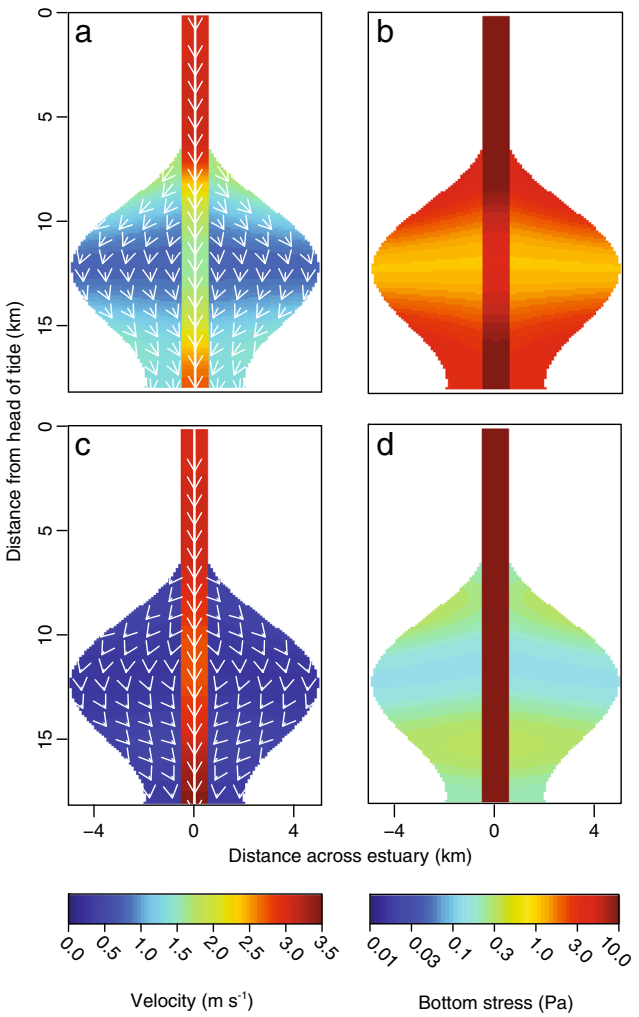

Fig. 10 Hydrodynamic model output showing water velocity (*left*) and bottom stress (*right*) in the central channel (6 m deep) and lateral shoals (1.5 m) at peak ebb tide with river flow comparable to the September 2011 flood (20,000 m^3 s^{-1}). The *top panels* represent the case without SAV on the shoal and the *bottom panels* are for the case with SAV

qualitatively suggests that nitrogen concentrations were greater than normal after 2011. Furthermore, differences in dissolved nutrients in response to increased inputs may not have been be detected because of rapid nutrient assimilation associated with algal and plant growth (Malone et al. 1996). We infer that dissolved nutrient loading during the flood event did not likely cause elevated nutrient concentrations in the bed because water residence time in the upper Chesapeake Bay during high-flow events is relatively short. As a result, dissolved nutrients generally pass through the region with little assimilation (Schubel and Pritchard 1986). However, decomposition of particulate organic nitrogen and desorption of particulate phosphorous can increase concentrations of pore water ammonium and phosphate (e.g., Kemp et al. 1984; Romero et al. 2006) and sloughing of organic epiphytic material during high flows can further add to the sediment nutrient pool (Fonseca et al. 1982). Resuspension events can enhance the rate of nutrient flux from the seabed to the water column through release of pore water solutes (Tengberg et al. 2003; Ståhlberg et al. 2006) and, thus, fuel algal growth. Conversely, the decrease in Chl *a* during the summer of 2012 and 2013 could be linked to decreased sediment resuspension and associated dissolved nutrient flux to the water column (Madsen et al. 2001). Furthermore, plant nutrient uptake (Cornelisen and Thomas 2006) and enhanced denitrification (Caffrey and Kemp 1990; Risgaard-Petersen et al. 2000) with increased water residence time inside the plant bed (Nixon et al. 1996; Lara et al. 2012) may also have decreased nutrient concentrations and, therefore, algal production.

Resistance to High Flows

River discharge during the 2011 flood event exceeded 20,000 m^3 s^{-1}, a value surpassed only three times previously since monitoring of Susquehanna River flow began in the late 1800s. While mechanical plant breakage, dislodgement, or scour and associated uprooting due to high flows likely caused substantial plant loss (Preen et al. 1995; Fonseca and Bell 1998), our analyses and model simulations suggest that the bed was also resilient to high flows by attenuating currents and shunting flow around the shoal and into surrounding channels.

The amount of force required to break or dislodge plants is highly variable depending on SAV species and sediment composition (Schutten et al. 2005), making the relative role of these processes difficult to assess. Our model simulations do suggest, however, that sediment scour, root exposure, and associated plant uprooting could have occurred, perhaps in conjunction with breakage or dislodging. Generally, bottom shear stresses that are greater than ~0.1 to 0.3 Pa result in sediment movement at a rate that depends on the difference between the applied stress and the threshold stress (Allen 1985). When modeled river flow was 20,000 m^3 s^{-1}, bottom stresses across a substantial area of the southern region of the flats exceeded this threshold (Fig. 10d), indicating incipient scour. In addition, although the modeled bottom stresses responsible for sediment transport were relatively small, the total drag forces were quite large, comparable to shear stresses simulated in our "no-SAV" scenario (Fig. 10b). These total stresses (about 3 Pa) were borne primarily by the plants, which might have been selectively broken or dislodged. Once thinning of the plant bed started for any reason, the system would tend toward unstable behavior. Any local loss of the protective SAV barrier would lead to greater local sediment scour, which in turn would lead to further plant loss, and so on. It is, therefore, possible that unstable plant loss and sediment scour associated with strong currents may have resulted in uprooting that caused large areas of plant loss during the flood. The increases in velocity and bottom stress were likely focused in the

southern region of the model domain both because of the constriction in width, and because maximum ebb tidal currents increase from north to south to conserve tidal volume transport. In addition, when the ebbing tide combined with southward river flow, velocity further accelerated in the southern region, thereby increasing bottom stress.

Our results also suggest that the plant bed attenuated flow during the flood event, as shown by relationships between the spatial distribution of plant loss and river discharge during high flow years. For example, the decreasing probability of plant loss with increasing distance from the outer edge of the plant bed (Fig. 3a) implies that inner regions of the bed were protected during flood events. The analysis also showed that as river discharge increased, the probability of loss at any given distance into the bed increased, suggesting that at higher flow rates, this protective capacity decreases. For these reasons, larger plant beds are generally more resilient to storm events because their inner core is protected (Gruber et al. 2011; Orth et al. 2012).

Model simulations support the idea the inner bed was sheltered from high flows. Bottom stresses on the shoal for the case without SAV were well above the threshold required to erode and transport sandy sediments (Fig. 10a, b); however, bottom stresses were near or below this threshold when SAV were present, particularly in the widest part of the shoal (Fig. 10c, d). This occurs because in addition to attenuating turbulence in the vertical dimension, canopy drag also dissipates the horizontal transfer of momentum from the leading edge toward the center of a plant bed (Luhar et al. 2008). Furthermore, the plant bed diverts flow from the shoal into the channel, resulting in decreased velocities on the shoal and acceleration of currents in the channel (Gambi et al. 1990; Chen et al. 2007; Luhar and Nepf 2013).

Recovery Following Loss

In addition to serving as a mechanism of resistance to disturbance, we suggest that positive feedback processes are also important for this bed's recovery. The region of higher turbidity around the edge of the plant bed during high tide (Fig. 9b) suggests that particles are transported into the bed with the rising tide. However, the large area of low turbidity outside the bed during low (Fig. 9c) tide implies that clear water drains out of the bed with the ebbing tide, creating the clear water "plume" evident in the aerial photograph (Fig. 9a). Because PLW inside the plant bed and in the plume region is greater than the minimum light required for plant survival (13 % of surface irradiance), recovery in this region is likely limited by the rate at which the plants can expand clonally or establish satellite colonies from fragments and seedlings. Light levels below this threshold at sites outside of the plume suggest that inadequate light could limit recovery in this region. However, if we use turbidity and Chl *a* data from the plume region to calculate PLW at the southernmost transect sites (1.5 m deep), light at the bottom would be 17 %, exceeding the minimum threshold. If the plume of clear water expands into deeper water as the bed expands southward, this process of a local feedback effect "spilling over" into adjacent regions could be a key mechanism for the bed's recovery to its prestorm extent.

Inferences About Recent and Historical Weather Events

Although sediment scour and poor water clarity associated with the September 2011 flood event were likely the primary drivers of plant loss, it is worth noting that decreased plant production in spring 2011 compared to 2010 (Fig. 5a, b) may have weakened the plant bed's ability to withstand the flood. With precipitation in March 2011 greater than six times above average, elevated turbidity that spring (Fig. 6a) likely decreased PLW (Fig. 5d), and thus, also plant production (Alcoverro et al. 1999; Longstaff and Dennison 1999). In addition, below average water temperatures in April 2011 could have delayed plant germination and further decreased plant production (McFarland and Shafer 2008), rendering the bed more susceptible to loss in the face of additional turbidity pulses (Cabello-Pasini et al. 2002; Yaakub et al. 2014; Fraser et al. 2014).

In addition, the inferences developed herein may help explain historical patterns of SAV abundance. In 1972, precipitation in the Susquehanna River watershed during Tropical Storm Agnes generated a 100- to 200-year flood that destroyed nearly the entire Susquehanna Flats SAV bed, with only sparse regrowth for several decades (Bayley et al. 1978; Kemp et al. 2005; Gurbisz and Kemp 2014). Based on the observed effects of the 2011 flood event, the magnitude of flooding likely exceeded the capacity of the bed to attenuate flow in 1972, leading to catastrophic plant loss. In fact, in a model run with comparable river flow (30,000 $m^3 s^{-1}$), bottom stresses on the vegetated shoal ranged from 0.3 to 0.7 Pa (not shown), values that lie within or surpass the threshold range for sediment motion. It is also possible that the 1972 bed was less dense than the 2011 bed, considering its trajectory of decline prior to Tropical Storm Agnes (Bayley et al. 1978; Kemp et al. 2005) and therefore less capable of attenuating and diverting flows. The seasonal timing of the 1972 storm also likely exacerbated bed damage because storms that occur near peak plant biomass are generally more destructive to SAV than those that occur after (Wang and Linker 2005). With presumably more sediment deposition and plant loss compared to the 2011 flood, resuspension in the absence of vegetation likely generated turbid conditions for an extended period of time, leading to a self-reinforcing bare-sediment state (Scheffer et al. 1993).

Concluding Comments

These analyses suggest that the ultimate effect of a flood event on submersed plant populations depends on the balance between mechanisms of plant loss and resilience, which involve complex biological, physical, and chemical interactions between a plant bed and its environment. In this case, although there was substantial SAV loss in response to a major flood event, the system was also remarkably resilient, apparently owing to strong biophysical feedback processes carried out by a large, dense, healthy SAV bed. Future work should aim to quantify threshold river flow rates beyond which plant beds cannot recover as well as the extent to which bed size and previous disturbances affect the tipping point. Whether genetic diversity interacts with these processes to enhance resilience is another important focus for additional research.

This paper also demonstrates how synthetic analysis of diverse datasets can be used to address ecological questions (Carpenter et al. 2009). We followed synthesis methods similar to those outlined in Kemp and Boynton (2011). For example, initial plots of data across time and space allowed for visualization of relevant patterns and trends. This preliminary information was then used to guide statistical approaches for more in-depth analysis. In addition, a simulation model was helpful for analyzing mechanisms and providing surrogates for missing but important variables. While alone, individual datasets may not be particularly meaningful, together and in the context of theory and other studies, they can be used to construct compelling explanatory models for ecological phenomena.

Acknowledgments We thank Debbie Hinkle, Steve Suttles, Laura Murray, and Steven Di Falco for help collecting samples; Viacheslav Lyubchich for guidance on statistical methods; Keith Williams and staff from NorthBay Adventure for field support; and two anonymous reviewers for constructive comments on an earlier version of the manuscript. WML, LPS, and CG received support to carry out this research from Maryland Sea Grant under awards NA10OAR4170072 R/SV-1 and NA14OAR4170090 R/SD-1 from the National Oceanic and Atmospheric Administration, U. S. Department of Commerce. This paper is contribution no. 5167 of the University of Maryland Center for Environmental Science Horn Point Laboratory and 3518 of the Virginia Institute of Marine Science, The College of William and Mary.

References

Alcoverro, T., R.C. Zimmerman, D.G. Kohrs, and R.S. Alberte. 1999. Resource allocation and sucrose mobilization in light-limited eelgrass Zostera marina. *Marine Ecology Progress Series* 187: 121–131. doi:10.3354/meps187121.

Allen, J.R.L. 1985. *Principles of physical sedimentology*. London: George Allen & Unwin Ltd.

Barbier, E.B., S.D. Hacker, C. Kennedy, E.W. Koch, A.C. Stier, and B.R. Silliman. 2011. The value of estuarine and coastal ecosystem services. *Ecological Monographs* 81: 169–193. doi:10.1890/10-1510.1.

Bartoli, M., D. Nizzoli, G. Castaldelli, and P. Viaroli. 2008. Community metabolism and buffering capacity of nitrogen in a *Ruppia cirrhosa* meadow. *Journal of Experimental Marine Biology and Ecology* 360: 21–30. doi:10.1016/j.jembe.2008.03.005.

Bayley, S., V.D. Stotts, P.F. Springer, and J. Steenis. 1978. Changes in submerged aquatic macrophyte populations at the head of Chesapeake Bay, 1958–1975. *Estuaries* 1: 171–182.

Blackburn, R.D., J.M. Lawrence, and D.E. Davis. 1961. Effects of light intensity and quality on the growth of *Elodea densa* and *Heteranthera dubia*. *Weeds* 9: 251–257.

Cabaço, S., R. Santos, and C.M. Duarte. 2008. The impact of sediment burial and erosion on seagrasses: a review. *Estuarine, Coastal and Shelf Science* 79: 354–366. doi:10.1016/j.ecss.2008.04.021.

Cabello-Pasini, A., C. Lara-Turrent, and R.C. Zimmerman. 2002. Effect of storms on photosynthesis, carbohydrate content and survival of eelgrass populations from a coastal lagoon and the adjacent open ocean. *Aquatic Botany* 74: 149–164. doi:10.1016/S0304-3770(02)00076-1.

Caffrey, J.M., and W.M. Kemp. 1990. Nitrogen cycling in sediments with estuarine populations of *Potamogeton perfoliatus* and *Zostera marina*. *Marine Ecology Progress Series* 66: 147–160.

Caffrey, J.M., M.C. Murrell, K.S. Amacker, J.W. Harper, S. Phipps, and M.S. Woodrey. 2014. Seasonal and inter-annual patterns in primary production, respiration, and net ecosystem metabolism in three estuaries in the northeast Gulf of Mexico. *Estuaries and Coasts* 37(51): 222–241.

Campbell, S., and L.J. McKenzie. 2004. Flood related loss and recovery of intertidal seagrass meadows in southern Queensland, Australia. *Estuarine, Coastal and Shelf Science* 60: 477–490. doi:10.1016/j.ecss.2004.02.007.

Cardoso, P.G., D. Rafaelli, A.I. Lillebø, T. Verdelhos, and M.A. Pardal. 2008. The impact of extreme flooding events and anthropogenic stressors on the macrobenthic communities' dynamics. *Estuarine, Coastal and Shelf Science* 76: 353–365.

Carpenter, S.R., N.F. Caraco, D.L. Correll, R.W. Howarth, V.H. Sharpley, and V.H. Smith. 1998. Nonpoint pollution of surface waters with phosphorous and nitrogen. *Ecological Applications* 8: 559–568.

Carpenter, S.R., E.V. Armbrust, P.W. Arzerberger, S.F. Chapin III, J.J. Elser, E.J. Hackett, A.R. Ives, P.M. Kareiva, M.A. Leibold, P. Lundberg, M. Mangel, N. Merchant, W.W. Murdoch, M.A. Palmer, D.P.C. Peters, S.T.A. Pickett, K.K. Smith, D.H. Wall, and A.S. Zimmerman. 2009. Accelerate synthesis in ecology and environmental sciences. *BioScience* 59(8): 699–701.

Chen, S., L.P. Sanford, E.W. Koch, F. Shi, and E.W. North. 2007. A nearshore model to investigate the effects of seagrass bed geometry on wave attenuation and suspended sediment transport. *Estuaries and Coasts* 30: 296–310.

Cloern, J.E. 2001. Our evolving conceptual model of the coastal eutrophication problem. *Marine Ecology Progress Series* 210: 223–253. doi:10.3354/meps210223.

Cornelisen, C., and F. Thomas. 2006. Water flow enhances ammonium and nitrate uptake in a seagrass community. *Marine Ecology Progress Series* 312: 1–13. doi:10.3354/meps312001.

Costanza, R., R. D'Arge, R. DeGroot, S. Farber, M. Grasso, B. Hannon, K. Limbrug, S. Naeem, R.V. O'Neil, J. Paruelo, R.G. Raskin, P. Sutton, and M. van den Belt. 1997. The value of the world's ecosystem services and natural capital. *Nature* 387: 253–260.

De Boer, W.F. 2007. Seagrass–sediment interactions, positive feedbacks and critical thresholds for occurrence: a review. *Hydrobiologia* 591: 5–24. doi:10.1007/s10750-007-0780-9.

Dennison, W.C., R.J. Orth, K.A. Moore, J.C. Stevenson, V. Carter, S. Kollar, P.W. Bergstrom, and R.A. Batiuk. 1993. Assessing water quality with submersed aquatic vegetation: habitat requirements as barometers of Chesapeake Bay health. *BioScience* 43: 86–94.

Diaz, R.J., and R. Rosenberg. 2008. Spreading dead zones and consequences for marine ecosystems. *Science* 321: 926–929. doi:10.1126/science.1156401.

Duffy, J.E., P.L. Reynolds, C. Bostrom, J.A. Coyer, M. Cusson, S. Donadi, J.G. Douglass, J.S. Eklof, A.H. Engelen, B.K. Eriksson, S. Fredriksen, L. Gamfeldt, C. Gustafsson, G. Hoarau, M. Hori, K. Hovel, K. Iken, J.S. Lefcheck, P. Moksnes, M. Nakaoka, M.I. O'Connor, J. Olsen, J.P. Richardson, J.L. Ruesink, E.E. Sotka, J. Thormar, M.A. Whalen, and J.J. Stachowicz. 2015. Biodiversity mediates top-down control in eelgrass ecosystems: a global comparative-experimental approach. *Ecology Letters* 19(7): 696–705. doi:10.1111/ele.12448.

Efron, B. 1987. Better bootstrap confidence intervals. *Journal of the American Statistical Association* 82(397): 171–185.

Fagherazzi, S., P.L. Wiberg, and A.D. Howard. 2003. Tidal flow field in a small basin. *Journal of Geophysical Research* 108: 1–10. doi:10.1029/2002JC001340.

Folke, C. 2006. Resilience: the emergence of a perspective for social–ecological systems analyses. *Global Environmental Change* 16: 253–267. doi:10.1016/j.gloenvcha.2006.04.002.

Fonseca, M.S., and S.S. Bell. 1998. Influence of physical setting on seagrass landscapes. *Marine Ecology Progress Series* 171: 109–121.

Fonseca, M. S., J. S. Fisher, J. C. Zieman, and G. W. Thayer. 1982. Influence of the seagrass, *Zostera marina L.*, on current flow. Estuarine, Coastal and Shelf Science 15: 351–364. doi:10.1016/0272-7714(82)90046-4.

Fraser, M.W., G.A. Kendrick, J. Statton, R.K. Hovey, A. Zavala-Perez, and D.I. Walker. 2014. Extreme climate events lower resilience of foundation seagrass at edge of biogeographical range. *Jounal of Ecology* 102: 1528–1536. doi:10.1111/1365-2745.12300.

Gambi, M.C., A.R.M. Nowell, and P.A. Jumars. 1990. Flume observations on flow dynamics in *Zostera marina* (eelgrass) beds. *Marine Ecology Progress Series* 61: 159–169. doi:10.3354/meps061159.

Granata, T., T. Serra, J. Colomer, X. Casamitjana, C.M. Duarte, and E. Gacia. 2001. Flow and particle distributions in a nearshore seagrass meadow before and after a storm. *Marine Ecology Progress Series* 218: 95–106. doi:10.3354/meps218095.

Grilo, T.F., P.G. Cardoso, M. Dolbeth, M.D. Bordalo, and M.A. Pardal. 2011. Effects of extreme climate events on the macrobenthic communities' structure and functioning of a temperate estuary. *Marine Pollution Bulletin* 62(2): 303–311. doi:10.1016/j.marpolbul.2010.10.010.

Gruber, R.K., and W.M. Kemp. 2010. Feedback effects in a coastal canopy-forming submersed plant bed. *Limnology and Oceanography* 55: 2285–2298. doi:10.4319/lo.2010.55.6.2285.

Gruber, R.K., D.C. Hinkle, and W.M. Kemp. 2011. Spatial patterns in water quality associated with submersed plant beds. *Estuaries and Coasts* 34: 961–972. doi:10.1007/s12237-010-9368-0.

Gurbisz, C., and W.M. Kemp. 2014. Unexpected resurgence of a large submersed plant bed in Chesapeake Bay: analysis of time series data. *Limnology and Oceanography* 59: 482–494. doi:10.4319/lo.2014.59.2.0482.

Harley, M.T., and S. Findlay. 1994. Photosynthesis-irradiance relationships for three species of submersed macrophytes in the tidal freshwater Hudson River. *Estuaries* 17: 200–205.

Hosmer, D.W., and S. Lemeshow. 2000. *Applied logistic regression*. New York: John Wiley & Sons, Inc.

Howarth, R.W., M. Hayn, R.M. Marino, N. Ganju, K. Foreman, K. McGlathery, A.E. Giblin, P. Berg, and J.D. Walker. 2013. Metabolism of a nitrogen-enriched coastal marine lagoon during the summertime. *Biogeochemistry* 118: 1–20. doi:10.1007/s10533-013-9901-x.

Intergovernmental Panel on Climate Change (IPCC), 2014. Climate Change 2014: Impacts, adaptation, and vulnerability. Part A: global and sectoral aspects. Contribution of Working Group II to the Fifth Assessment Report of the Intergovernmental Panel on Climate Change [Field, C.B., V.R. Barros, D.J. Dokken, K.J. Mach, M.D. Mastrandrea, T.E. Bilir, M. Chatterjee, K.L. Ebi, Y.O. Estrada, R.C. Genova, B. Girma, E.S. Kissel, A.N. Levy, S. MacCracken, P.R. Mastrandrea, and L.L. White (eds.)]. Cambridge University Press, Cambridge, United Kingdom and New York, NY, USA, 1132 pp.

Jackson, J.B., M.X. Kirby, W.H. Berger, K.A. Bjorndal, L.W. Botsford, B.J. Bourque, R.H. Bradbury, R. Cooke, J. Erlandson, J.A. Estes, T. Pl Hughes, S. Kidwell, C.B. Lange, H.S. Lenihan, J.M. Pandolfi, C.H. Peterson, R.S. Steneck, M.J. Tegner, and R.R. Warner. 2001. Historical overfishing and the recent collapse of coastal ecosystems. *Science* 293: 629–637. doi:10.1126/science.1059199.

Kemp, W.M., and W.R. Boynton. 2011. Synthesis in estuarine and coastal ecological research: what is it, why is it important, and how do we teach it? *Estuaries and Coasts* 35(1): 1–22.

Kemp, W.M., W.R. Boynton, R.R. Twilley, J.C. Stevenson, and L.G. Ward. 1984. Influences of submersed vascular plants on ecological processes in upper Chesapeake Bay. In *The estuary as a filter*, ed. V.S. Kennedy, 367–394. New York: Academic Press, Inc.

Kemp, W.M., R. Batiuk, R. Bartleson, P. Bergstrom, V. Carter, C.L. Gallegos, W. Hunley, L. Karrh, E.W. Koch, J.M. Landwher, K.A. Moore, L. Murray, M. Naylor, N.B. Rybicki, J.C. Stevenson, and D.J. Wilcox. 2004. Habitat requirements for submerged aquatic vegetation in Chesapeake Bay: water quality, light regime, and physical-chemical factors. *Estuaries* 27: 363–377.

Kemp, W.M., W.R. Boynton, J.E. Adolf, D.F. Boesch, W.C. Boicourt, G. Brush, J.C. Cornwell, T.R. Fisher, P.M. Glibert, J.D. Hagy, L.W. Harding, E.D. Houde, D.G. Kimmel, W.D. Miller, R.I.E. Newell, M.R. Roman, E.M. Smith, and J.C. Stevenson. 2005. Eutrophication of Chesapeake Bay: historical trends and ecological interactions. *Marine Ecology Progress Series* 303: 1–29.

Koch, E.W. 2001. Beyond light: Physical, geological, and geochemical parameters as possible submersed aquatic vegetation habitat requirements. *Estuaries* 24: 1–17.

Laird, N.M., and J.H. Ware. 1982. Random-effects models for longitudinal data. *Biometrics* 38: 963–974.

Lande, R., and S. Shannon. 1996. The role of genetic variation in adaptation and population persistence in a changing environment. *Evolution* 50: 434–437.

Lara, M., G. Peralta, J.J. Alonso, E.P. Morris, V. González-Ortiz, J.J. Rueda-Márquez, and J.L. Pérez-Lloréns. 2012. Effects of intertidal seagrass habitat fragmentation on turbulent diffusion and retention time of solutes. *Marine Pollution Bulletin* 64: 2471–2479. doi:10.1016/j.marpolbul.2012.07.044.

Longstaff, B.J., and W.C. Dennison. 1999. Seagrass survival during pulsed turbidity events: the effects of light deprivation on the seagrasses *Halodule pinifolia* and *Halophila ovalis*. *Aquatic Botany* 65: 105–121. doi:10.1016/S0304-3770(99)00035-2.

Lotze, H., H.S. Lenihan, B.J. Borque, R.H. Bradbury, R.G. Cooke, M.C. Kay, S.M. Kidwell, M.X. Kirby, C.H. Peterson, and J.B.C. Jackson. 2006. Depletion, degradation, and recovery potential of estuaries and coastal seas. *Science* 312(5781): 1806–1809.

Luhar, M., and H.M. Nepf. 2013. From the blade scale to the reach scale: a characterization of aquatic vegetative drag. *Advances in Water Resources* 51: 305–316. doi:10.1016/j.advwatres.2012.02.002.

Luhar, M., J. Rominger, and H. Nepf. 2008. Interaction between flow, transport and vegetation spatial structure. *Environmental Fluid Mechanics* 8: 423–439. doi:10.1007/s10652-008-9080-9.

Madsen, J.D., P.A. Chambers, W.F. James, E.W. Koch, and D.F. Westlake. 2001. The interaction between water movement, sediment dynamics and submersed macrophytes. *Hydrobiologia* 444: 71–84.

Malone, T.C., D.J. Conley, T.R. Fisher, P.M. Glibert, L.W. Harding, and K.G. Sellner. 1996. Scales of nutrient-limited phytoplankton productivity in Chesapeake Bay. *Estuaries and Coasts* 19(2b): 371–385.

Mariotti, G., and S. Fagherazzi. 2013. A two-point dynamic model for the coupled evolution of channels and tidal flats. *Journal of Geophysical Research, Earth Surface* 118: 1387–1399. doi:10.1002/jgrf.20070.

Maxwell, P.S., K.A. Pitt, D.D. Burfeind, A.D. Olds, R.C. Babcock, and R.M. Connolly. 2014. Phenotypic plasticity promotes persistence following severe events: physiological and morphological responses of seagrass to flooding. *Journal of Ecology* 102: 54–64. doi:10.1111/1365-2745.12167.

McFarland, D.G., and D.J. Shafer. 2008. Factors influencing reproduction in American wild celery: a synthesis. *Journal of Aquatic Plant Management* 46: 129–144.

McGlathery, K.J., K. Sundbäck, and I.C. Anderson. 2007. Eutrophication in shallow coastal bays and lagoons: the role of plants in the coastal filter. *Marine Ecology Progress Series* 348: 1–18. doi:10.3354/meps07132.

Middelboe, A.L., and S. Markager. 1997. Depth limits and minimum light requirements of freshwater macrophytes. *Freshwater Biology* 37: 553–568.

Moore, K.A. 2004. Influence of seagrasses on water quality in shallow regions of the lower Chesapeake Bay. *Journal of Coastal Research* 45: 162–178.

Moore, K.A., Richard L. Wetzel, and Robert J. Orth. 1997. Seasonal pulses of turbidity and their relations to eelgrass (*Zostera marina L.*) survival in an estuary. *Journal of Experimental Marine Biology and Ecology* 215: 115–134. doi:10.1016/S0022-0981(96)02774-8.

Moore, K.A., D.J. Wilcox, and R.J. Orth. 2000. Analysis of the abundance of submersed aquatic vegetation communities in the Chesapeake Bay. *Estuaries* 23(1): 115–127.

Najjar, R.G., C.R. Pyke, M.B. Adams, D. Breitburg, C. Hershner, W.M. Kemp, R. Howarth, M.R. Mulholland, M. Paolisso, D. Secor, K. Sellner, D. Wardrop, and R. Wood. 2010. Potential climate-change impacts on the Chesapeake Bay. *Estuarine, Coastal and Shelf Science* 86: 1–20. doi:10.1016/j.ecss.2009.09.026.

Nixon, S.W., J.W. Ammerman, L.P. Atkinson, V.M. Berounsky, G. Billen, W.C. Boicourt, W.R. Boynton, T.M. Church, D.M. Ditoro, R. Elmgren, H.J. Garber, A.E. Giblin, R.A. Jahnke, N.J.P. Owens, M.E.Q. Pilson, and S.P. Seitzinger. 1996. The fate of nitrogen and phosphorus at the land-sea margin of the North Atlantic Ocean. *Biogeochemistry* 35: 141–180.

Orth, R.J., M.L. Luckenbach, S.R. Marion, K.A. Moore, and D.J. Wilcox. 2006. Seagrass recovery in the Delmarva Coastal Bays, USA. *Aquatic Botany* 84(1): 26–36.

Orth, R.J., M.R. Williams, S.R. Marion, D.J. Wilcox, T.J.B. Carruthers, K.A. Moore, W.M. Kemp, W.C. Dennison, N. Rybicki, P. Bergstrom, and R.A. Bauiuk. 2010. Long-term trends in submersed aquatic vegetation (SAV) in Chesapeake Bay, USA, related to water quality. *Estuaries and Coasts* 33: 1144–1163. doi:10.1007/s12237-010-9311-4.

Orth, R.J., K.A. Moore, S.R. Marion, D.J. Wilcox, and D.B. Parrish. 2012. Seed addition facilitates eelgrass recovery in a coastal bay system. *Marine Ecology Progress Series* 448: 177–195.

Palinkas, C.M., J.P. Halka, M. Li, L.P. Sanford, and P. Cheng. 2013. Sediment deposition from tropical storms in the upper Chesapeake Bay: field observations and model simulations. *Continental Shelf Research* 86: 6–16. doi:10.1016/j.csr.2013.09.012.

Parsons, T.R., Y. Maita, and C.M. Lalli. 1984. *A manual of chemical and biological methods for seawater analysis*. Oxford: Pergamon Press.

Peterson, C.H., R.A. Luettich Jr., F. Micheli, and G.A. Skilleter. 2004. Attenuation of water flow inside seagrass canopies of differing structure. *Marine Ecology Progress Series* 268: 81–92.

Pinheiro, J.C., and D.M. Bates. 2000. *Mixed effects models in S and S-Plus*. New York: Springer-Verlag.

Preen, A. R., W. J. Lee Long, and R. G. Coles. 1995. Flood and cyclone related loss, and partial recovery, of more than 1000 km2 of seagrass in Hervey Bay, Queensland, Australia. Aquatic Botany 52. Elsevier: 3–17. doi:10.1016/0304-3770(95)00491-H.

Ralph, G.M., R.D. Seitz, R.J. Orth, K.E. Knick, and R.N. Lipcius. 2013. Broad-scale association between seagrass cover and juvenile blue crab density in Chesapeake Bay. *Marine Ecology Progress Series* 488: 51–63. doi:10.3354/meps10417.

Rappaport, D.J., and W.G. Whitford. 1999. How ecosystems respond to stress. *Bioscience* 49: 193–203. doi:10.2307/1313509.

Reusch, T.B.H., A. Ehlers, A. Hämmerli, and B. Worm. 2005. Ecosystem recovery after climatic extremes enhanced by genotypic diversity. *Proceedings of the National Academy of Sciences of the United States of America* 102: 2826–2831. doi:10.1073/pnas.0500008102.

Risgaard-Petersen, N., L. Ditlev, and M. Ottosen. 2000. Nitrogen cycling in two temperate Zostera marina beds: seasonal variation. *Marine Ecology Progress Series* 198: 93–107.

Romero, J., K.S. Lee, M. Perez, M.A. Mateo, and T. Alcoverro. 2006. Nutrient dynamics in seagrass ecosystems. In *Seagrasses: biology, ecology, and conservation*, ed. A.W.D. Larkum, R.J. Orth, and C.M. Duarte, 227–254. The Netherlands: Springer.

Rybicki, N.B., and J.M. Landwehr. 2007. Long-term changes in abundance and diversity of macrophyte and waterfowl populations in an estuary with exotic macrophytes and improving water quality. *Limnology and Oceanography* 52(3): 1195–1207.

Sanford, L.P. 1994. Wave-forced resuspension of upper Chesapeake Bay muds. *Estuaries* 17: 148–165. doi:10.1007/BF02694911.

Sanford, L.P. 2008. Modeling a dynamically varying mixed sediment bed with erosion, deposition, bioturbation, consolidation, and armoring. *Computers & Geosciences* 34: 1263–1283.

Scheffer, M., S.H. Hosper, M.L. Meijer, B. Moss, and E. Jeppesen. 1993. Alternative equilibria in shallow lakes. *Trends in Ecology & Evolution* 8: 275–279.

Schubel, J.R., and D.W. Pritchard. 1986. Responses of upper Chesapeake Bay to variations in discharge of the Susquehanna River. *Estuaries* 9: 236–249.

Schutten, J., J. Dainty, and A.J. Davy. 2005. Root anchorage and its significance for submerged plants in shallow lakes. *Journal of Ecology* 93: 556–571. doi:10.1111/j.1365-2745.2005.00980.x.

Sculthorpe, C.D. 1967. *The biology of aquatic vascular plants*. London: Edward Arnold.

Ståhlberg, C., D. Bastviken, B.H. Svensson, and L. Rahm. 2006. Mineralisation of organic matter in coastal sediments at different frequency and duration of resuspension. *Estuarine, Coastal and Shelf Science* 70: 317–325. doi:10.1016/j.ecss.2006.06.022.

Tengberg, A., E. Almroth, and P. Hall. 2003. Resuspension and its effects on organic carbon recycling and nutrient exchange in coastal sediments: In situ measurements using new experimental technology. *Journal of Experimental Marine Biology and Ecology* 285–286: 119–142. doi:10.1016/S0022-0981(02)00523-3.

Tomasko, D.A., C.A. Corbett, H.S. Greening, and G.E. Raulerson. 2005. Spatial and temporal variation in seagrass coverage in Southwest Florida: assessing the relative effects of anthropogenic nutrient load reductions and rainfall in four contiguous estuaries. *Marine Pollution Bulletin* 50: 797–805. doi:10.1016/j.marpolbul.2005.02.010.

Twilley, R.R., W.M. Kemp, K.W. Staver, J.C. Stevenson, and W.R. Boynton. 1983. Nutrient enrichment of estuarine submersed vascular plant communities. 1. Algal growth and effects on production of plants and associated communities. *Marine Ecology Progress Series* 23: 179–191.

Van der Heide, T., E.H. van Nes, M.M. van Katwijk, H. Olff, and A.J.P. Smolders. 2011. Positive feedbacks in seagrass ecosystems—evidence from large-scale empirical data. *PloS One* 6, e16504. doi:10.1371/journal.pone.0016504.

Walker, D.I., G.A. Kendrick, and A.J. McComb. 2006. Decline and recovery of seagrass ecosystems—the dynamics of change. In

Seagrasses: biology, ecology, and conservation, ed. A. Larkum, R.J. Orth, and C. Duarte, 551–565. The Netherdlands: Springer.

Wang, P., and L. C. Linker. 2005. Effect of timing of extreme storms on Chesapeake Bay submerged aquatic vegetation. In Hurricane Isabel in perspective, ed. K. G. Sellner, Edgewater, MD: Chesapeake Research Consortium Publication 05–160.

Ward, L.G. 1985. The influence of wind waves and tidal currents on sediment resuspension in middle Chesapeake Bay. *Geo-Marine Letters* 5: 71–75.

Yaakub, S.M., E. Chen, T.J. Bouma, P.L.A. Erftemeijer, and P.A. Todd. 2014. Chronic light reduction reduces overall resilience to additional shading stress in the seagrass *Halophila ovalis*. *Marine Pollution Bulletin* 83: 467–474. doi:10.1016/j.marpolbul.2013.11.030.